



Effects of charging and doping on orbital hybridizations and distributions in TiO₂ clusters

Hong Min Zhao^{a,d}, Miao Miao Wu^{b,d}, Qian Wang^{c,d,*}, Puru Jena^d

^a Department of Physics, School of Science, Beijing Jiaotong University, Beijing 100044, China

^b Department of Advanced Materials and Nanotechnology, College of Engineering, Peking University, Beijing 100871, China

^c Center for Applied Physics and Technology, College of Engineering, Peking University, Beijing 100871, China

^d Department of Physics, Virginia Commonwealth University, Richmond, VA 23284, USA

ARTICLE INFO

Article history:

Received 17 June 2011

Accepted 25 August 2011

Available online 30 August 2011

Keywords:

Cluster

Charge transfer

Orbital hybridization

ABSTRACT

Charging and doping are two important strategies used in TiO₂ quantum dots for photocatalysis and photovoltaics. Using small clusters as the prototypes for quantum dots, we have carried out density functional calculations to study the size-specific effects of charging and doping on geometry, electronic structure, frontier orbital distribution, and orbital hybridization. We find that in neutral (TiO₂)_n clusters the charge transfer from Ti to O is almost size independent, while for the anionic (TiO₂)_n clusters the corresponding charge transfer is reduced but it increases with size. When one O atom is substituted with N, the charge transfer is also reduced due to the smaller electron affinity of N. As the cluster size increases, the populations of 3d and 4s orbitals of Ti decrease with size, while the populations of the 4p orbital increase, suggesting size dependence of spd hybridizations. The present study clearly shows that charging and doping are effective ways for tailoring the energy gap, orbital distributions, and hybridizations.

© 2011 Elsevier B.V. All rights reserved.

1. Introduction

The amount of energy necessary to sustain our society is ever increasing as the population of the world increases. Since the supply of fossil fuels is very limited and they have had an adverse effect on the environment, it is imperative to explore new energy sources, which are abundant, renewable, secure, clean, safe, and cost-effective. The Sun is our only external energy source, harnessing its energy has been one of the main objectives in renewable energy research. There are many ways to convert solar radiation directly into electrical power or chemical fuel; silicon solar cell is such an example [1–3]. However, the capital cost of such devices is not suitable for large-scale applications. One of the attractive strategies is to use quantum dots based structures to mimic photosynthesis in the conversion and storage of solar energy [4–6]. Among the widely used quantum dots, titanium dioxide (TiO₂), due to its chemical stability, low-cost, and nontoxicity, has been extensively used in photovoltaic solar cells and photo-electrochemical devices [7–10]. To improve the efficiency, two strategies are widely used: dye-sensitizing and doping. In dye sensitized TiO₂ quantum dots, electrons are injected to the dot

from the photo-excited dye, which is a dynamic charging process. When employing the doping strategy, transition metals are not suitable due to problems associated with thermal instability and carrier-recombination. Non-metal doped TiO₂ was found to be effective for improving the photosensitivity of TiO₂ in the visible light region. Currently research is focused on non-metal doping. Asahi et al. [11] first carried out substitutional N doping in TiO₂ by the sputtering method and found that photosensitivity in the visible spectral range can be enhanced. Since then, N-doping is widely used in TiO₂ nano-particles, nano-tubes, films, and powders [12–15]. In practical applications of TiO₂ quantum dots, the environment such as substrate, dye molecules, and the linkers also have important influence on their structure and properties. To get fundamental insight into the effects of charging and doping on TiO₂ quantum dot, we studied small TiO₂ clusters, which can be used as prototypes for quantum dots, nano-particles, and powders. We recall that previous studies on small oxide clusters have demonstrated that they can be treated as embryonic forms of their crystals [16,17]. Our focus is on the study of the effects of charging and doping on orbital hybridizations and distributions, while the previous studies have mainly concentrated on the effect of cluster size on geometry and energy gap. Mowbray et al. [18] studied theoretically the stability and electronic properties of (TiO₂)₅ cluster with and without B and N doping. In this study, we address the following basic issues by studying the stability and electronic properties of (TiO₂)_n ($n < 5$) clusters and their anions

* Corresponding author at: Center for Applied Physics and Technology, College of Engineering, Peking University, Beijing 100871, China. Tel./fax: +86 10 62752043.
E-mail address: qianwang2@pku.edu.cn (Q. Wang).

with and without N doping: How do the geometry, orbital hybridizations and orbital distributions change when a charge or a dopant is introduced to a TiO_2 quantum dot? How do the changes depend on the dot size?

2. Computational details

Calculations are carried out using the density functional theory (DFT) with BPW91 functional [19,20] for the exchange–correlation potential, as implemented in Gaussian03 [21] program. The 6-31+G* basis sets for Ti and 6-311++G** [22–25] basis sets for O and N were used. The validity of our theoretical procedure is tested by calculating electron ionization potential (IP) of Ti atom and electron affinities (EA) of O atom. These are found to be 6.92 and 1.57 eV, respectively, and are in good agreement with corresponding experimental values of 6.83 and 1.46 eV [26,27]. The calculated adiabatic detachment energy (ADE) and vertical detachment energy (VDE) for TiO_2 molecule are 1.49 and 1.58 eV, respectively, which also agree well with the corresponding experimental values of 1.59 and 1.59 eV [28]. In our calculations all the geometries of neutrals and their anions for doped and undoped clusters are fully optimized without any symmetry constraint. The relative stabilities of the structural isomers are discussed based on their energies.

3. Results and discussion

3.1. Neutral and anionic $(\text{TiO}_2)_n$ clusters

In Figs. 1 and 2 we show the structures of the ground state and some selected low lying isomers of neutral and single charged anionic $(\text{TiO}_2)_n$ clusters, respectively. The following features are noticed: (1) For $n=1, 2, 3,$ and 4 , the ground state geometries of the neutral and its anion have the same symmetry and similar geometric configuration, but the bonds in the anions are elongated due to the extra electron, especially for $n=4$. Here the elongated bonds make the anion less compact as compared to the neutral one even though both of them have the same C_{2v} symmetry, labeled as $C_{2v,a}$ and $C_{2v,b}$ respectively. (2) For the neutral cluster of $(\text{TiO}_2)_2$, the ground state geometry has C_{2h} symmetry and the C_{2v} isomer is 0.3 eV higher in energy. When one electron is introduced, the energy difference between these two isomers is

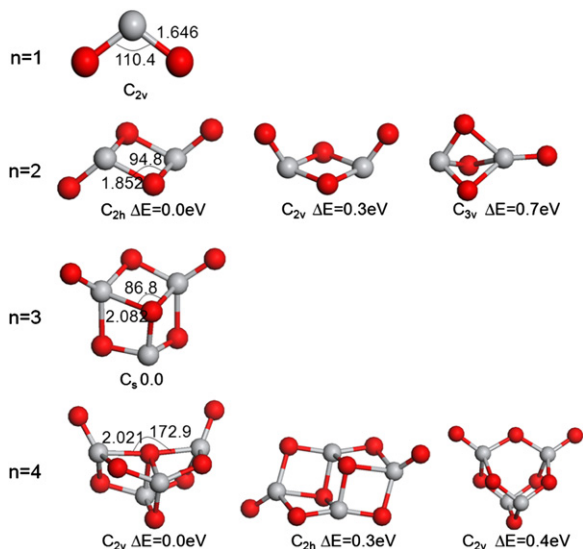


Fig. 1. Optimized geometries of neutral $(\text{TiO}_2)_n$ clusters for the low-lying isomers.

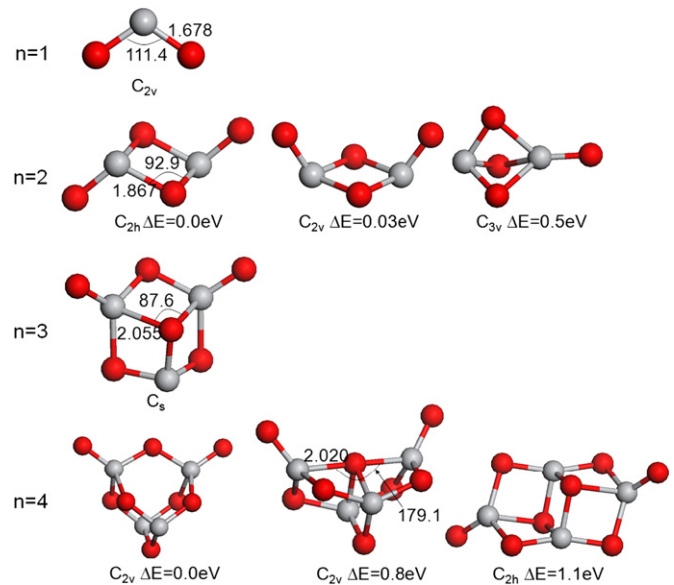


Fig. 2. Optimized geometries of anionic $(\text{TiO}_2)_n^-$ clusters for the low-lying isomers.

	Neutral HOMO	Neutral LUMO	Anion HOMO	Anion LUMO
n=1				
n=2				
n=3				
n=4				

Fig. 3. Distributions of frontier orbitals of the neutral and anionic $(\text{TiO}_2)_n^-$.

reduced to just 0.03 eV. This agrees well with the value of 0.02 eV calculated by Li and Dixon. [29] at the CCSD(T) level. Since both C_{2h} and C_{2v} isomers have open geometry, addition of the negative charge induces near degeneracy in the anion. The situation is different for $n=4$, where the ground state geometry of the neutral is $C_{2v,a}$, and the isomers C_{2h} and $C_{2v,b}$ are 0.3 and 0.4 eV higher in energy, respectively. Once negatively charged, the isomer $C_{2v,b}$ becomes the ground state, and the isomer $C_{2v,a}$ is 0.8 eV higher in energy. This is in agreement with the result obtained by Qu et al. for the $(\text{TiO}_2)_4$ anion [30]. In this case, addition of the negative charge increases the energy difference between structural isomers. Therefore, the effect of charging on geometry depends on the geometric details of isomers.

In order to get some in depth understanding of the electronic structure and its effect on the geometries, we have analyzed the distributions of frontier orbitals. Fig. 3 shows the highest occupied molecular orbital (HOMO) and the lowest unoccupied molecular orbital (LUMO) of the neutral and anionic $(\text{TiO}_2)_n$ clusters ($n=1, 2, 3,$ and 4). Following features are seen: (1) The HOMOs of the neutral clusters are mainly contributed by 2 orbitals of oxygen while the LUMOs are dominated by the contributions of Ti. However, the orbital compositions are size dependent.

For $n=1$, the 4s–3d hybridized orbitals contribute to the LUMO, while starting for $n \geq 2$, the 3d_{z²} orbital is predominant. (2) When an electron is introduced, the LUMO of the neutral cluster becomes the HOMO of the anion. This is why the LUMO of the neutral and HOMO of the anion are quite similar. Although the LUMOs of the anions are derived from the orbitals of Ti, the details are different depending on the size. For example, the main components for $n=2$ are 3d_{z²} orbitals of Ti, while for $n=3$ and 4, the main contribution is from the 3d_{x²-y²} of Ti.

As we know the electronic configuration of an isolated Ti atom is 3d²4s²4p⁰. This is changed in (TiO₂)_n clusters for two main reasons: the charge transfer to O and the spd hybridizations. The details are given in Fig. 4. In Fig. 4(a) we plot the orbital occupation of Ti in neutral Ti(O₂)_n clusters while the corresponding values for the two spins are given in Fig. 4(b) and (c). The general trend is that as the size increases, the occupation of 3d and 4s orbitals decreases, while that of the 4p orbital increases.

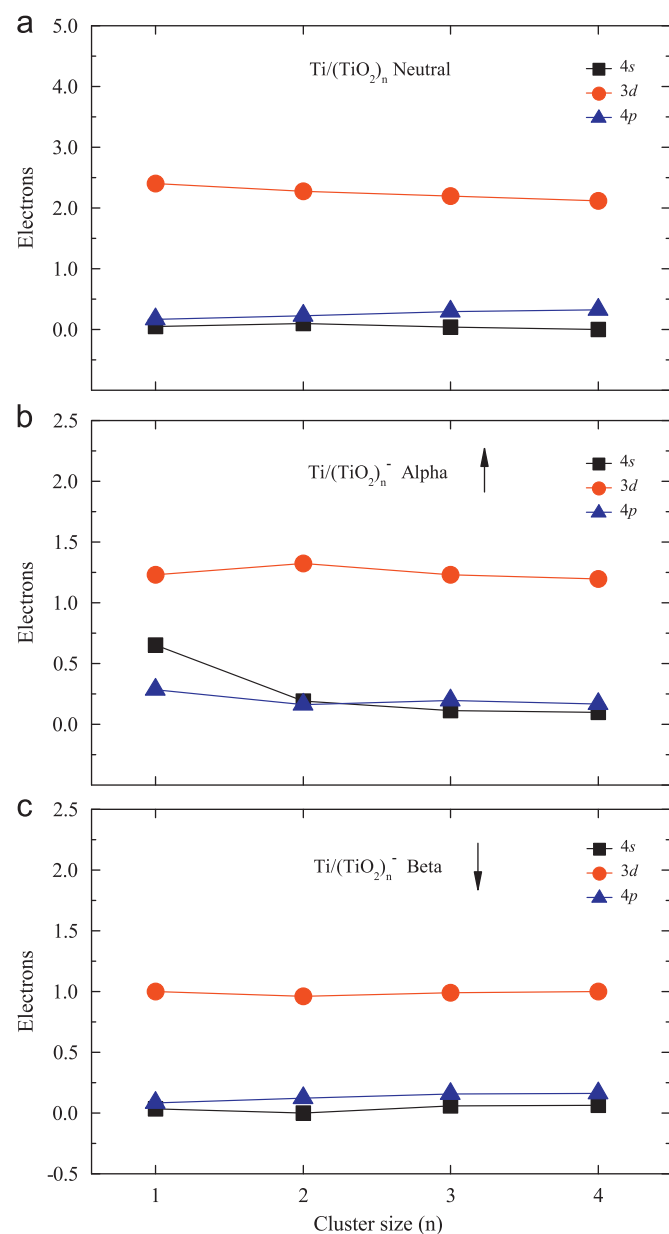


Fig. 4. Changes of orbital populations with size for (a) neutral (TiO₂)_n and (b, c) anionic (TiO₂)_n⁻ clusters.

3.2. Ti_nO_{2n-1}N clusters and their anions

We now consider replacing one of the O atoms with N atom. Since, N atom has one electron less than that of O atom, when one O atom is replaced by one N atom in (TiO₂)_n, the number of electrons is reduced. In this sense, N doping is equivalent to hole doping. However, because of the difference in electron affinity and atomic size between N and O, N doping brings more complexity as compared to pure hole injection. In order to search for the most stable doping site, we have performed extensive calculations by replacing O with N from all the non-equivalent sites in the neutral and anionic clusters. The resulting ground state geometries are given in Figs. 5 and 6, respectively. We have found that N atom prefers to occupy the high coordination site binding with Ti. Doping causes some changes in geometry. Compared with the Ti–O bond of the neutral, the Ti–N bond length is increased by 0.06 Å for $n=1$ and 0.05 Å for $n=2$, while decreased by 0.08 Å for $n=3$. For $n=4$, N atom was not at the symmetric site for Ti atoms, and the symmetry changed from C_{2v} to C_s. The Ti–N bond lengths are found to be 2.038 Å and 1.968 Å. The bond angles of O–Ti–N are reduced by 4.1° and 3.1° for $n=1$ and 2, while increased by 2.9° and 2.6° for $n=3$ and 4, respectively.

For the anions, the Ti–N bond length increased by 0.07 Å for $n=1$ and 0.06 Å for $n=4$, while decreased by 0.03 Å for $n=2$. For $n=3$, reflecting very small change. The bond angles of O–Ti–N decrease for $n=1$ and 4, while they increase for $n=2$ and 3. The corresponding changes are 6.7°, 1.2°, 3.6°, and 0.5° for $n=1, 2, 3$, and 4, respectively.

To study the effect of doping on the electronic structure, we plot the HOMOs and LUMOs of the doped neutrals and anions in Fig. 7. These can be compared with the results in Ti_nO_{2n} (see Fig. 3) to probe their similarity and the difference. For the un-doped Ti_nO_{2n} clusters, the LUMO of neutral is very similar to the HOMO of anion, while the situation is changed for the doped cluster (Ti_nO_{2n-1}N). Actually they are quite different. For example, for neutral TiON, the LUMO is mainly from the 2p orbitals of O and N, while the HOMO of the anion is mainly contributed by the orbitals of Ti. The HOMO of neutral Ti_nO_{2n} is similar to that of Ti_nO_{2n-1}N⁻ anion, since Ti_nO_{2n-1}N⁻ anion has the same number of electrons as the neutral Ti_nO_{2n}. This is also true for the LUMO, i.e., the LUMO of anionic Ti_nO_{2n-1}N⁻ is very similar to the LUMO of neutral Ti_nO_{2n}. Doping not only changes the orbital hybridizations and distributions, but also significantly reduces the HOMO–LUMO gap from 2.48, 3.30, 2.10, and 3.01 eV in (TiO₂)_n to 1.32, 1.18, 0.25, and 0.32 eV in Ti_nO_{2n-1}N for $n=1, 2, 3$, and 4, respectively.

Fig. 8 shows the changes of average orbital populations of Ti with respect to cluster size for the N-doped neutrals and anions. They share similar behavior with the un-doped clusters, namely,

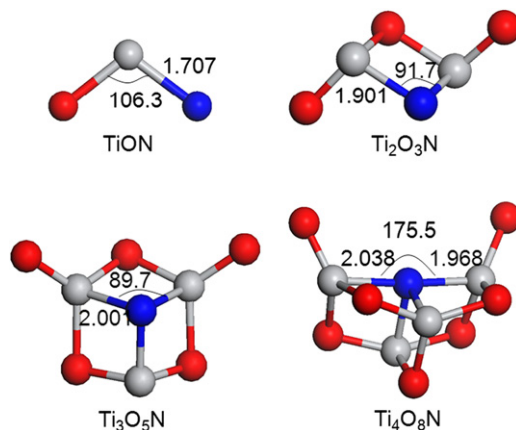


Fig. 5. Optimized geometries of the N-doped neutral Ti_nO_{2n-1}N clusters.

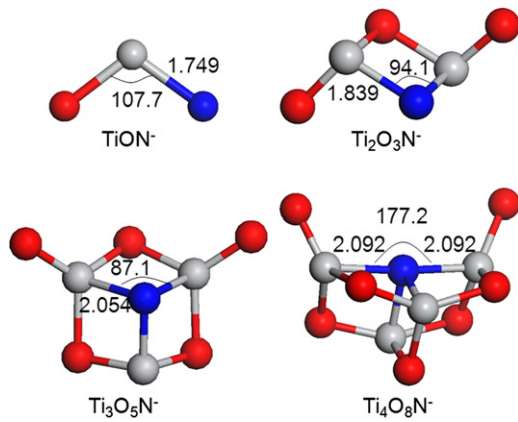


Fig. 6. Optimized geometries of the N-doped anionic $Ti_nO_{2n-1}N^-$ clusters.

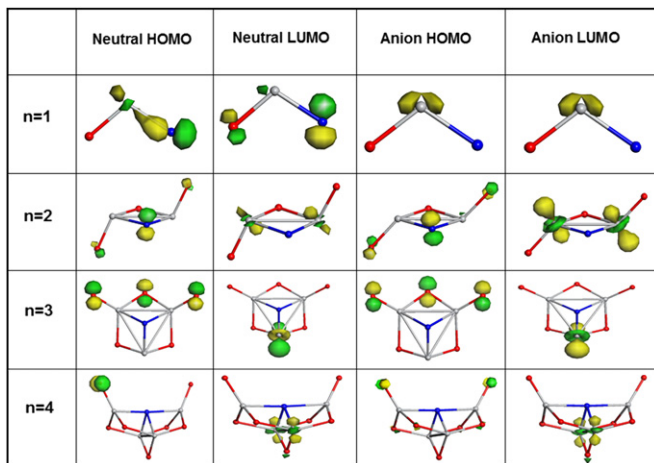


Fig. 7. Distributions of frontier orbitals of the neutral and anionic $Ti_nO_{2n-1}N$.

the populations on 3d and 4s orbitals decrease with size, while the populations on 4p orbital increase.

To get a quantitative picture of the charge transfer, we list in Table 1 the average charges on Ti site and charges on N site in the neutral and anionic $(TiO_2)_n$ clusters with and without N doping. We can clearly see the effect of the charge and doping on charge transfer and charge distributions. For the neutral $(TiO_2)_n$, the average charges on Ti atoms are 1.43, 1.43, 1.40, and 1.44e for $n=1, 2, 3$, and 4, respectively, reflecting almost no size dependence. When negatively charged, the corresponding values become 0.72, 0.87, 1.25, and 1.32e. This is because the introduced charge reduces the electron withdrawing ability of the O sites. Such an effect becomes weak as the cluster size increases, which makes the average charges on Ti sites to gradually increase. When one O atom is substituted with N, due to the lesser electron affinity of N atom, charge transfer is weakened. When the size n goes from 1 to 4, the average charges on Ti sites are found to be 1.16, 1.26, 1.26, and 1.33e. They are further reduced to 0.47, 1.20, 1.21, and 1.28e when the cluster is negatively charged. The charges on N site also increase with the size n for the neutral doped clusters, and small oscillations exist in the negatively charged ones.

4. Conclusion

In summary, using the density functional theory, we have discussed the effects of charging and doping on orbital hybridizations and distributions in small TiO_2 clusters, which can be

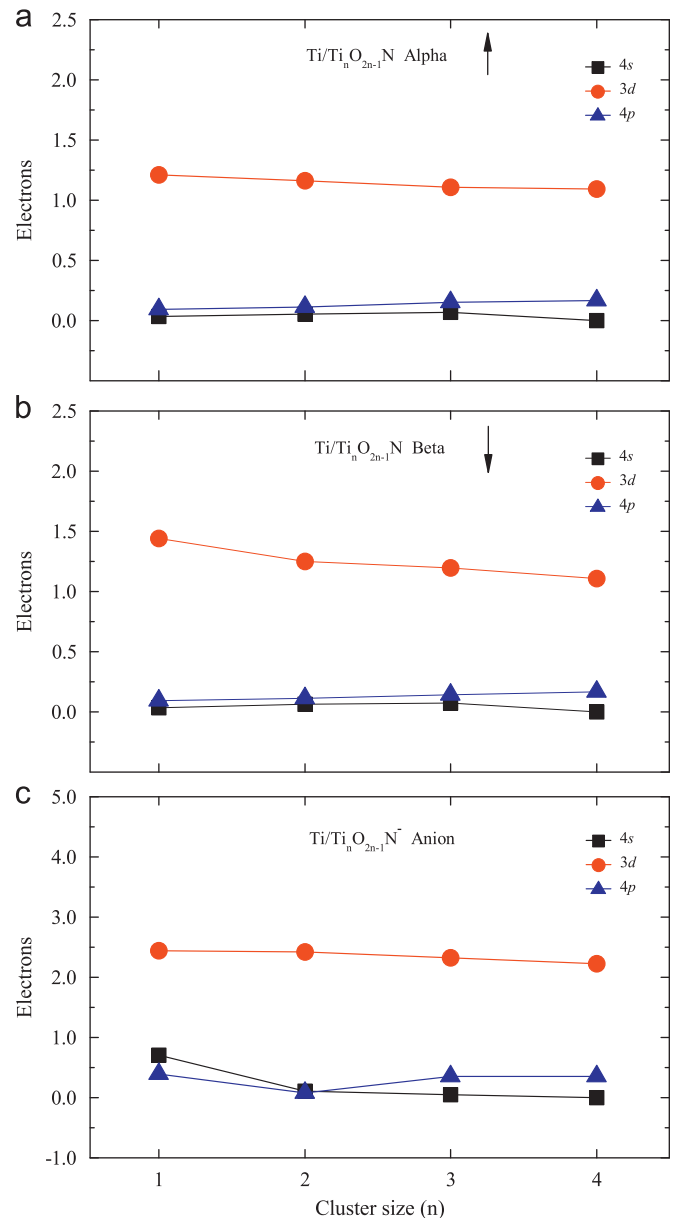


Fig. 8. Changes of orbital populations with size for the N-doped neutral (a and b for spin up \uparrow and spin down \downarrow , respectively) and anionic (c) $Ti_nO_{2n-1}N$.

Table 1

Average charges (e) on Ti site and charges (e) on N site in the neutral and anionic $(TiO_2)_n$ clusters with and without N doping.

Undoped	Ave. chg./Ti	Doped	Ave. chg./Ti	Chg./N
TiO_2	1.43	$TiON$	1.16	-0.50
TiO_2^-	0.72	$TiON^-$	0.47	-0.68
Ti_2O_4	1.43	Ti_2O_3N	1.26	-0.56
$Ti_2O_4^-$	0.87	$Ti_2O_3N^-$	1.20	-0.88
Ti_3O_6	1.40	Ti_3O_5N	1.26	-0.72
$Ti_3O_6^-$	1.25	$Ti_3O_5N^-$	1.21	-0.79
Ti_4O_8	1.44	Ti_4O_7N	1.33	-0.78
$Ti_4O_8^-$	1.32	$Ti_4O_7N^-$	1.28	-0.78

regarded as prototypes of TiO_2 quantum dots. However, as mentioned before, in the practical applications of TiO_2 quantum dots, the environment such as substrates, dye molecules, and the linkers will have important influence on the geometries and properties. The situations would be much more complicated as

compared to the free standing condition used in our present study. For example the charge transfer from dye molecules to the quantum dot is an instant and dynamic process, here we treat it statically. We show that once the system is charged, the orbital hybridizations and distributions will be significantly changed. This information is helpful for further understanding the dynamic phenomena happening in the practical environment.

Acknowledgment

This work is partially supported by grants from the US Department of Energy. This research used resources of the National Energy Research Scientific Computing Center, which is supported by the Office of Science of the US Department of Energy under Contract No. DE-AC02-05CH11231.

References

- [1] R.M. Swanson, S.K. Beckwith, R.A. Crane, W.D. Eades, Y.H. Kwark, R.A. Sinton, S.E. Swirhun, *IEEE Trans. Electron Devices* 31 (1984) 661.
- [2] R.A. Sinton, Y. Kwark, J.Y. Gan, R.M. Swanson, *IEEE Electron Device Lett.* 7 (1986) 567.
- [3] W. Wetzling, *Sol. Energy Mater. Sol. Cells* 38 (1995) 487.
- [4] A. Marti, L. Cuadra, A. Luque, *IEEE Trans. Electron. Devices* 48 (2001) 2394.
- [5] A. Luque, A. Marti, N. Lopez, E. Antolin, E. Canovas, C. Stanley, C. Farmer, L.J. Caballero, L. Cuadra, J.L. Balenzategui, *Appl. Phys. Lett.* 87 (2005) 3.
- [6] A. Luque, A. Marti, A.J. Nozik, *MRS Bull.* 32 (2007) 236.
- [7] K. Kalyanasundaram, M. Gratzel, *Coord. Chem. Rev.* 177 (1998) 347.
- [8] S.A. Haque, Y. Tachibana, R.L. Willis, J.E. Moser, M. Gratzel, D.R. Klug, J.R. Durrant, *J. Phys. Chem. B* 104 (2000) 538.
- [9] M. Gratzel, *Prog. Photovoltaics* 8 (2000) 171.
- [10] K. Shankar, J. Bandara, M. Paulose, H. Wietasch, O.K. Varghese, G.K. Mor, T.J. LaTempa, M. Thelakkat, C.A. Grimes, *Nano Lett.* 8 (2008) 1654.
- [11] R. Asahi, T. Morikawa, T. Ohwaki, K. Aoki, Y. Taga, *Science* 293 (2001) 269.
- [12] L. Dong, Y. Ma, Y.W. Wang, Y.T. Tian, G.T. Ye, X.L. Jia, G.X. Cao, *Mater. Lett.* 63 (2009) 1598.
- [13] E. Camps, L. Escobar-Alarcon, M.A. Camacho-Lopez, D.A.S. Casados, *Mater. Sci. Eng. B—Adv. Funct. Solid-State Mater.* 174 (2010) 80.
- [14] C. Burda, Y.B. Lou, X.B. Chen, A.C.S. Samia, J. Stout, J.L. Gole, *Nano Lett.* 3 (2003) 1049.
- [15] Y. Nosaka, M. Matsushita, J. Nishino, A.Y. Nosaka, *Sci. Technol. Adv. Mater.* 6 (2005) 143.
- [16] B.V. Reddy, P. Jena, *Chem. Phys. Lett.* 288 (1998) 253.
- [17] Q. Sun, B.K. Rao, P. Jena, D. Stolcic, Y.D. Kim, G. Gantefor, A.W. Castleman, *J. Chem. Phys.* 121 (2004) 9417.
- [18] D.J. Mowbray, J.I. Martinez, J.M.G. Lastra, K.S. Thygesen, K.W. Jacobsen, *J. Phys. Chem. C* 113 (2009) 12301.
- [19] A.D. Becke, *Phys. Rev. A* 38 (1988) 3098.
- [20] Y. Wang, J.P. Perdew, *Phys. Rev. B* 43 (1991) 8911.
- [21] M.J. Frisch, G.N. Trucks, H.B. Schlegel, et al., GAUSSIAN 03, Revision B.04, Gaussian, Inc., Pittsburgh, PA, 2003.
- [22] R. Krishnan, J.S. Binkley, R. Seeger, J.A. Pople, *J. Chem. Phys.* 72 (1980) 650.
- [23] V.A. Rassolov, J.A. Pople, M.A. Ratner, T.L. Windus, *J. Chem. Phys.* 109 (1998) 1223.
- [24] M.M. Francl, W.J. Pietro, W.J. Hehre, J.S. Binkley, M.S. Gordon, D.J. Defrees, J.A. Pople, *J. Chem. Phys.* 77 (1982) 3654.
- [25] T. Clark, J. Chandrasekhar, G.W. Spitznagel, P.V. Schleyer, *J. Comput. Chem.* 4 (1983) 294.
- [26] J.E. Sohl, Y. Zhu, R.D. Knight, *J. Opt. Soc. Am. B* 7 (1990) 9.
- [27] H. Hotop, W.C. Lineberger, *J. Phys. Chem. Ref. Data* 14 (1985) 731.
- [28] H.B. Wu, L.S. Wang, *J. Chem. Phys.* 107 (1997) 8221.
- [29] S.G. Li, D.A. Dixon, *J. Phys. Chem. A* 112 (2008) 6646.
- [30] Z.W. Qu, G.J. Kroes, *J. Phys. Chem. B* 110 (2006) 8998.